Early Antiangiogenic Activity of SU11248 Evaluated *In vivo* by Dynamic Contrast-Enhanced Magnetic Resonance Imaging in an Experimental Model of Colon Carcinoma

Pasquina Marzola,[1] Anna Degrassi,[2] Laura Calderan,[1] Paolo Farace,[1] Elena Nicolato,[1] Caterina Crescimanno,[1] Marco Sandri,[1] Anna Giusti,[2] Enrico Pesenti,[2] Andrea Terron,[2] Andrea Sbarbati,[1] and Francesco Osculati[1]

Abstract

Purpose: To compare two dynamic contrast-enhanced magnetic resonance imaging (DCE-MRI) techniques in terms of their ability in assessing the early antiangiogenic effect of SU11248, a novel selective multitargeted tyrosine kinase inhibitor, that exhibits direct antitumor and antiangiogenic activity via inhibition of the receptor tyrosine kinases platelet-derived growth factor receptor, vascular endothelial growth factor receptor, KIT, and FLT3.

Experimental Design: A s.c. tumor model of HT29 human colon carcinoma in athymic mice was used. Two DCE-MRI techniques were used based, respectively, on macromolecular [Gd-diethylenetriaminepentaacetic acid (DTPA)-albumin] and low molecular weight (Gd-DTPA) contrast agents. The first technique provided a quantitative measurement of transendothelial permeability and fractional plasma volume, accepted surrogate markers of tumor angiogenesis. With the second technique, we quantified the initial area under the concentration-time curve, which gives information related to tumor perfusion and vascular permeability. Experiments were done before and 24 hours after a single dose administration of SU11248.

Results: The early antiangiogenic effect of SU11248 was detected by DCE-MRI with macromolecular contrast agent as a 42% decrease in vascular permeability measured in the tumor rim. The effect was also detected by DCE-MRI done with Gd-DTPA as a 31% decrease in the initial area under the concentration-time curve. Histologic slices showed a statistically significant difference in mean vessel density between the treated and control groups.

Conclusions: The early antiangiogenic activity of SU11248 was detected *in vivo* by DCE-MRI techniques using either macromolecular or low molecular weight contrast agents. Because DCE-MRI techniques with low molecular weight contrast agents can be used in clinical studies, these results could be relevant for the design of clinical trials based on new paradigms.

Inhibition of angiogenesis is a relatively new strategy in the fight against cancer. Various angiogenesis inhibitors have been developed to target vascular endothelial cells and block tumor angiogenesis. More than 30 agents have entered clinical trials in cancer patients (1), although only one therapy based on angiogenic modulation, Avanstin (Bevacizumab, Genentech, South San Francisco, CA), a monoclonal antibody to vascular endothelial growth factor, has thus far shown sufficient clinical benefit to be approved. The evaluation of efficacy of antiangiogenic compounds is a challenge for preclinical and clinical research. The traditional criterion to assess response of a tumor to treatment is based on the measurement of tumor size reduction. However, vascular effects may precede, by a remarkably long time interval, the effect on tumor growth. For these reasons, testing of antiangiogenic compounds requires imaging methods that can detect early vascular alteration. Dynamic contrast-enhanced magnetic resonance imaging (DCE-MRI) techniques play a relevant role in this field (2, 3) due to their ability to detect morphologic and functional characteristics of tumor vasculature by the differential distribution of contrast agents in healthy and tumoral tissues. In clinical studies, DCE-MRI is done by using small molecular weight contrast agents [i.e., small Gd chelates as Gd-diethylenetriaminepentaacetic acid (DTPA)], although several preclinical studies have shown the advantages of high molecular weight contrast agents (4–6). Our group has recently reported the usefulness of DCE-MRI done with Gd-DTPA-albumin in the early detection of the efficacy of an antiangiogenic compound, specifically SU6668, in an experimental model of colon carcinoma (7). However, no macromolecular contrast agent is, at present, available for clinical applications even if a new class of contrast agents, namely ultrasmall superparamagnetic

Authors' Affiliations: [1]Dipartimento di Scienze Morfologico-Biomediche, Sezione di Anatomia ed Istologia, Università di Verona, Verona and [2]Nerviano Medical Sciences, Nerviano, Milan, Italy

Received 12/28/04; revised 5/2/05; accepted 5/16/05.

The costs of publication of this article were defrayed in part by the payment of page charges. This article must therefore be hereby marked *advertisement* in accordance with 18 U.S.C. Section 1734 solely to indicate this fact.

Requests for reprints: Pasquina Marzola, Dipartimento di Scienze Morfologico-Biomediche, Università di Verona, Strada Le Grazie 8, I-37134 Verona, Italy. Phone: 39-45-802-7255; Fax: 39-45-802-7163; E-mail: pasquina.marzola@univr.it.

doi:10.1158/1078-0432.CCR-04-2655

iron oxide particles, presents features similar to Gd-DTPA-albumin in DCE-MRI experiments (8), and are approaching clinical approval.

SU11248 is a novel selective multitargeted receptor tyrosine kinase inhibitor that exhibits direct antitumor activity against tumor cells dependent on signaling through platelet-derived growth factor receptor, KIT, FLT3, or vascular endothelial growth factor receptor for proliferation/survival (9–11). SU11248 also has antiangiogenic activity through its inhibition of vascular endothelial growth factor receptor and platelet-derived growth factor receptor signaling. In mouse xenograft models, SU11248 caused regression, growth arrest, or substantially reduced growth of various established xenografts derived from human (HT-29, A431, Colo205, H-460, SF763T, A375, and MDA-MB-435) or rat (C6) tumor cells (9). The antiangiogenic activity was evaluated in some representative experiments through the mean vessel density from histologic slices and using the Miles assay for vascular permeability (9). Decrease in mean vessel density was observed even in tumor models which did not regress after treatment. Moreover, histologic studies showed that, in some experimental models, SU11248 induced extensive destruction of tumor mass, although no evidence of regression of tumor size was obtained (9). These findings well illustrate the issues connected with the evaluation of the efficacy of novel antiangiogenic compounds in preclinical setups.

In this paper, we describe the use of two DCE-MRI techniques in the *in vivo* evaluation of the early antiangiogenic efficacy of SU11248. The antiangiogenic effect of SU11248 was shown by DCE-MRI done with a macromolecular prototype contrast agent (Gd-DTPA-albumin) using an experimental protocol widely applied in preclinical studies (7, 12); moreover, this effect was shown by DCE-MRI done with a clinically approved, low molecular weight contrast agent (Gd-DTPA), using an experimental protocol directly exportable to the clinical practice.

Materials and Methods

Animals and experimental model. Athymic *nu/nu* mice (Harlan, San Pietro, Italy) were housed in a ventilated, temperature-controlled room, with a 12-hour light/dark cycle. HT-29 human colon carcinoma fragments were implanted s.c. in the flank of 20 nude mice weighing ~25 g. Animals were inserted in the study when the tumors reached a weight of ~500 mg and were subdivided into two groups according to the MRI protocol, one group (n = 5 control and n = 5 treated) underwent DCE-MRI with macromolecular contrast agent, and another group (n = 5 control and n = 5 treated) underwent MRI with small molecular weight contrast agent (Gd-DTPA). All animals received a single dose (45 mg/kg, p.o.) of SU11248 (n = 10) or vehicle (n = 10) and were observed by MRI prior to and 24 hours after treatment. The investigation complied with the national legislation about the care and use of laboratory animals.

Contrast agents. Gd-DTPA-albumin, synthesized according to Ogan et al. (13), was obtained from R. Brasch (Contrast Media Laboratory, University of California, San Francisco, CA) and is characterized by an average molecular weight of 94 kDa, corresponding to ~45 molecules of Gd-DTPA covalently bound to each albumin molecule. A bolus of Gd-DTPA-albumin was injected into the tail vein at a dose of 30 μmol of Gd/kg; the total injected volume was 2.6 mL/kg. Gd-DTPA (Magnevist, Schering, Germany) was given in bolus trough the tail vein at a dose of 100 μmol/kg.

MRI. Mice were anaesthetized by inhalation of a mixture of air and O_2 containing 0.5% to 1% halothane and placed in prone position into a 3.5 cm i.d. transmitter-receiver birdcage coil. Images were acquired using a Biospec tomograph (Bruker, Karlsruhe, Germany) equipped with a 4.7 T, 33 cm bore horizontal magnet (Oxford Ltd., Oxford, United Kingdom). Coronal spin echo and transversal multislice, fast spin echo T2-weighted (RARE, TE_{eff} = 70 ms) were acquired for tumor localization and good visualization of extratumoral tissues. In experiments done with Gd-DTPA-albumin, a dynamic series of three-dimensional, transversal spoiled-gradient echo images were acquired with the following variables: repetition-time / echo-time = 50/3.5 ms, flip angle (α) = 90 degrees; matrix size, 128 × 64 × 32; field-of-view, 5 × 2.5 × 3 cm^3 (corresponding to 0.39 × 0.39 mm^2 in-plane resolution and 0.94 mm slice thickness); number of acquisition, 1. The acquisition time for a single three-dimensional image was 104 seconds; a dynamic scan of 24 images was acquired with 30-second time intervals between each image (total acquisition time, 53 minutes.). The contrast agent was injected in bolus during the time interval between the first and the second scan. The experimental protocol closely followed the one reported in ref. (12), with the modifications already described (7, 14). For experiments with Gd-DTPA, after coronal spin echo and transversal multislice, fast spin echo T2-weighted (RARE, TE_{eff} = 70 ms) images, acquired for tumor localization, a dynamic series of T1-weighted, spoiled gradient echo images were acquired with the following variables: repetition-time, 65 ms; echo-time, 3.8 ms; α = 90 degrees; matrix size, 128 × 256 zero-filled at 256 × 256; field-of-view, 6 × 6 cm^2; space resolution, 0.234 × 0.234 mm^2. Two slices (slice thickness, 1.5 mm and slice separation, 1.5 mm) were acquired at the tumor center. The acquisition time for a single image was 8.2 seconds and a time interval of 1 second was placed between two successive images (time resolution, 9.2 seconds). A total of 60 images were acquired, 3 before and 57 after the contrast medium bolus injection. The dynamic evolution of the signal was observed for about 10 minutes.

MR quantitative evaluation and statistics. After acquisition, data were transferred to a personal computer for analysis. Data were analyzed using MatLab 5.2 (The MathWorks, Inc., Natick, MA). Images acquired with Gd-DTPA-albumin were analyzed as previously reported (7, 14) in order to obtain values of transendothelial permeability (kPS) and fractional plasma volume (fPV) on a pixel-by-pixel basis or on regions of interest basis. In each animal, the central five slices of the three-dimensional data set were analyzed. Regions of interests were manually tracked to cover the tumor rim; a band ~2 mm wide at the periphery, on the external side of the tumor was considered as the rim. Quantitative analysis of MR images was limited to the tumor rim, due to scarce penetration of the contrast agent in the tumor core, data referred to the core are more prone to experimental errors (7). The signal in the rim was averaged and analyzed to obtain the mean kPS and fPV values in the rim of the selected slice. Images acquired with Gd-DTPA were analyzed using software programs developed in MatLab 5.2. Two regions of interest were manually selected to cover a band of ~2 mm in the tumor rim, on the external side of the tumor. The average signal intensity within each region of interest was calculated at each timepoint and normalized for the signal intensity of the standard. Signal intensity values were converted to Gd concentrations using the known expression of signal intensity for a gradient echo sequence. The area under the curve (AUC) was obtained by integrating the time dependence of the Gd concentration for the first 92 seconds after Gd-DTPA injection using a trapezoidal approximation of the curve. Statistical significance of the differences between pre- and posttreatment values was assessed using paired t test at the 95% confidence intervals.

Histologic and immunocytochemical methods. Animals belonging to the group examined at MRI with Gd-DTPA albumin were sacrificed after the last MRI examination and prepared for histology. Prior to removal of the tumor, a mark was made on the overlying skin with an ink pen, perpendicular to and in the midpoint of the cranial caudal axis of the tumor. After fixation in zinc fixative for 6 hours, the tumor was cut in half exactly along the marking line and embedded in paraffin. From each of

the two halves, five slices (5 μm thick) were taken. The sections obtained were in planes corresponding to those used for the MR images. Three of the five sections were stained with H&E; the remaining two were used for CD31 immunohistochemical staining of endothelial cells using a 1:800 dilution of CD31 (PharMingen, San Diego, CA; Rat A-mouse #557355) primary antibody incubated overnight. The resultant products were visualized with the 3,3′-diaminobenzidine chromogen. The primary antibody was replaced by rat nonimmune serum (DAKO, Carpinteria, CA; X0912) at the same protein concentration for negative controls.

Histologic image analysis. Sections stained with H&E showed a central necrotic area and a peripheral area with viable tumoral cells. For measuring the number of vessels, each slide was examined for four fields using a 10× objective (each field measuring 647 × 483 μm), selected in the viable area of the tumor as previously described (7). The image analysis program Image ProPlus 4.0 was used. Vessels were selected on color basis and, for each field, the number of positive objects was counted. Vessels located in the capsule and objects with area <10 μm^2 were excluded. The average area of vessels was measured within the same fields as before, using a 20× objective (each field measuring 323.7 × 241.8 μm). Each vessel was manually lined and area values were collected.

Results

DCE-MRI experiments done with Gd-DTPA-albumin were quantitatively evaluated as described in the previous section to obtain kPS and fPV values. Figure 1 quantitatively shows the effect of a single-dose administration of SU11248 on tumor mean plasma volume (fPV) and transendothelial permeability (kPS) measured in the tumor rim. A significant decrease in kPS (42%) was observed in the treated group, 24 hours after administration of a single dose of SU11248.

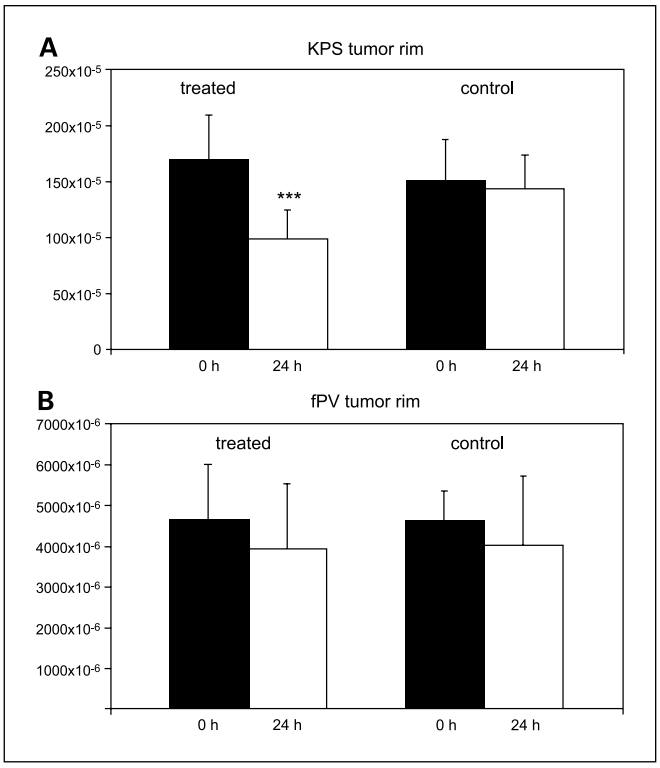

Fig. 1. Mean values of kPS (in mL/min/cm^3 of tissue) and fPV (in mL/cm^3 of tissue) in the tumor rim, prior to and 24 hours after administration of SU11248 or vehicle. Columns, mean; bars, ±SD; data are averaged over five central slices for each animal. Asterisks, statistical significance (***, $P < 0.001$).

This variable did not change in the control group. No significant alteration was observed in the fractional plasma volume both in the treated and control groups.

Figure 2 shows representative images acquired prior to, and 174 seconds after, injection of a bolus of Gd-DTPA, for one animal belonging to the treated group. Images were acquired before treatment; the enhancement in the signal intensity was more pronounced in the peripheral region of the tumor. Data were quantified by calculating the AUC for the first 92 seconds after contrast medium injection. Signal intensity values were measured in the tumor rim and converted to a concentration using a value of 4.5 mmol/L/s for the Gd-DTPA relaxivity. Average AUC values are reported in Fig. 3. A statistically significant decrease (31%) in the average AUC value is evident for the treated group of animals 24 hours after treatment. No decrease was observed for the control group. It is worthwhile to mention that 4.5 mmol/L/s is the relaxivity of Gd-DTPA measured in water at 0.5 T; it is well known that the relaxivity of contrast agents is dependent on the field intensity and on the medium. In particular, it changes significantly with the microviscosity of the medium which can alter the rotational correlation time of the Gd-containing molecules. We have previously reported that the relaxivity of Gd-DTPA increases by 200% when measured in aqueous solutions containing very high concentration of macromolecules (40% powder milk solution) compared with distilled water (14). Therefore, the relaxivity of Gd-DTPA in tumor tissue at 4.7 T is probably different from 4.5 mmol/L/s; nevertheless, this difference could introduce only a systematic error in the AUC values determined.

The ability of SU11248 to inhibit tumor angiogenesis was also evaluated by histology. Sections stained with H&E showed the presence of a central necrotic area and a peripheral zone with viable tumor cells. Histologic slices were quantitatively evaluated by counting vessels and their dimensions in the viable area. Table 1 reports results obtained by analysis of histologic slices from animals belonging to the treated and control groups. A statistically significant difference was observed in the number of vessels that was 30% lower in the treated compared with the control group. No alteration was observed in the dimensions of the vessels, quantified by the mean vessels area, perimeter, and diameter. No difference in the tumor size (either measured by caliper or by MR images) was appreciated after a single-dose administration of SU11248.

Discussion

The importance of DCE-MRI techniques in assessing the effect of antiangiogenic treatments has been shown by several experimental studies. Recently, DCE-MRI techniques have also been applied in clinical studies aimed at evaluating the efficacy of new antiangiogenic drugs (15). SU11248 is an oral selective multitargeted tyrosine kinase inhibitor that exhibits direct antitumor and antiangiogenic activity via inhibition of the receptor tyrosine kinases platelet-derived growth factor receptor, vascular endothelial growth factor receptor, KIT, and FLT3 and is currently in phase II oncology clinical trials (16). In this work, we have compared two DCE-MRI techniques based on macromolecular and small molecular weight contrast agents in terms of their capability to

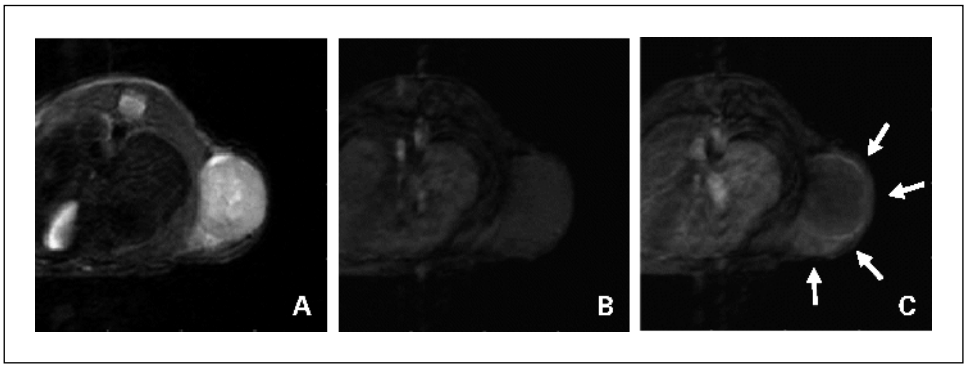

Fig. 2. T2w,T1w-pre-, and T1w-postcontrast transversal images acquired for an animal belonging to the treated group. *A,* T2w RARE image; *B,* T1w precontrast image; *C,* T1w postcontrast image acquired 104 seconds after injection of a bolus of Gd-DTPA (100 μmol/kg), the enhancement is particularly pronounced at the tumor rim (*arrows*).

establish the early efficacy of SU11248 on tumor vasculature. The first technique exploits the ability of a macromolecular contrast agent to probe the permeability of tumor vasculature to macromolecules as well as to measure the fractional plasma volume, and is based on the acquisition of images at the steady state concentration of the contrast agent (12). The second technique is based on the rapid acquisition of T1-weighted sequences probing the first passage of a small molecular weight contrast agent in the tumor tissue. Analysis of the time-dependence of signal intensity curve, which could be converted to a concentration curve, gives information related to tumor perfusion and vascular permeability when data are quantified by the initial area under the time-concentration curve (17). Several preclinical studies have shown that variables obtained from DCE-MRI done with macromolecular contrast agents correlates with the histologic grade of a tumor. This technique has been also applied for the detection of the efficacy of several antiangiogenic drugs in experimental models. Moreover, as DCE-MRI done with macromolecular contrast agents has fewer timing constraints compared with first passage techniques, it allows imaging of multiple tumors or multiple sections through a given tumor or imaging at higher space resolution (18). On the other hand, DCE-MRI techniques based on the acquisition of the first passage of small molecular weight contrast agents through the tumor tissue present the advantage of being applicable to clinical studies, being small molecular weight contrast agents extensively used in clinical practice from about 20 years.

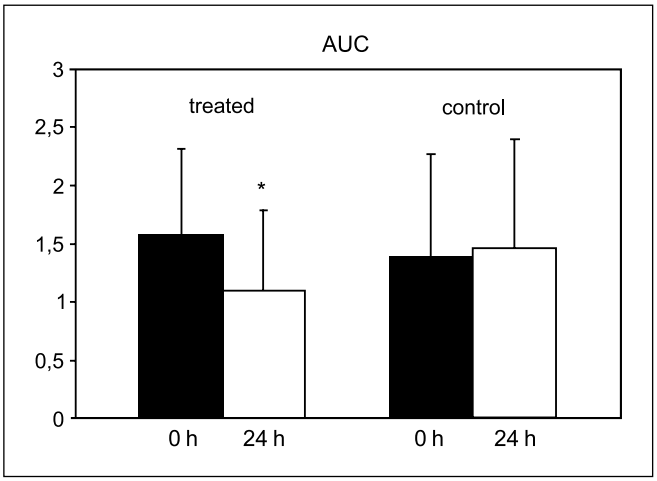

Fig. 3. Mean values of AUC, measured in the tumor rim, prior to and 24 hours after administration of SU11248 or vehicle. Columns, mean; bars, ±SD; data averaged over the two acquired slices. Asterisks, statistical significance (*, $P < 0.05$).

In this study, we have shown that DCE-MRI done with macromolecular contrast agents detects the early effect of SU11248 on tumor angiogenesis as a substantial decrease in the vascular permeability in the tumor rim. Within the first 24 hours after treatment, no effect of SU11248 on fractional plasma volume is detected. The last findings is surprising because histochemistry data detects a statistically significant difference in the mean vessel density (between treated and control groups). However, several papers have already shown discrepancies between MRI and mean vessel density data. Turetschek et al. have reported no statistically significant correlation between mean vessel density and fPV measured with Gd-DTPA-albumin or other contrast agents in a chemically induced experimental model of breast cancer (9, 19, 20). Fractional plasma volume determined using Gd-DTPA-albumin (21) or ultrasmall superparamagnetic iron oxide particles (22) was not found to be different in tumors treated with an inhibitor of the vascular endothelial growth factor receptor tyrosine kinases PTK787/ZK 222584, despite a significant decrease in mean vessel density detected in treated tumors. Drevs et al. (23) have reported that MRI acquisitions detected an increase in tumor blood volume after treatment with PKT787/ZK 222584 despite a reduced number of vessels; this was explained by virtue of hemodynamic dilation of the remaining vessels. In our case, no dilation of remaining vessels was observed by histologic measurement of average vessel area, suggesting that contrast-enhanced MRI is inherently sensitive to the sole perfused and functional vessels, whereas histologic analysis is sensitive to all the anatomically distinguishable vascular structures. In our previous work on the characterization of the early efficacy of SU6668, we have observed that the decrease in fPV, monitored by DCE-MRI after a single-dose administration, was accompanied by a significant difference between control and treated groups in both mean vessel density and mean vessels area, monitored by histology (7). In the present case, the percentage decrease in the mean vessel density (30%) was inferior but comparable to that observed in the SU6668 study (40%); however, the fractional plasma volume of a particular tissue depends on both mean vessel density and mean vessel area. Thus, even if the differences in mean vessel density were comparable, the total effect on fractional plasma volume was smaller, perhaps explaining the insensitivity of MRI to these alterations observed in the present investigation.

Table 1. CD31 immunohistochemical staining: microvessel density and mean area, perimeter, and diameter of vessels

	Number of vessels per field (mean ± SD)*	Mean area (mean ± SD), μm^2	Mean perimeter (mean ± SD), μm	Mean diameter (mean ± SD), μm
Treated	39.71 ± 16.62	340.99 ± 81.94	89.22 ± 15.12	8.90 ± 0.93
Control	55.79 ± 27.58	294.06 ± 87.13	84.26 ± 13.89	8.92 ± 1.59

*$P < 0.05$.

In the present study, attention was focused on an early time point (24 hours) in order to avoid confounding effects due the tumor evolution. It is known that, as tumors grow, vascularization also frequently decreases in untreated animals (24). When looking at the effect of a specific treatment comparing vascular characteristics of treated and control animals, the alterations due to volume growth could mask the effect due to the therapy; to overcome this problem, some studies have been done comparing tumors matched by size instead of comparing tumors matched by age (24). Our previous study done with SU6668 showed that the effect on angiogenesis was detectable by DCE-MRI at early time points (24 hours), whereas later (3, 7, and 14 days) the effect was masked by different patterns of evolution of tumoral and extratumoral vascularization (7). The importance of early response to antiangiogenic drugs, as detected by DCE-MRI experiments, and the fact that it is correlated with relevant clinical end points, such as tumor response and the extent of tumor shrinkage, has also been reported in a clinical study on PTK787/ZK 222584 (15). The early effect of SU11248 on tumor vasculature was also shown by DCE-MRI techniques done with a small molecular weight contrast agent. In fact, the AUC showed a statistically significant decrease 24 hours after treatment, whereas no significant decrease was observed in the control group. Signal intensity–time curve can be analyzed quantitatively to extract vascular permeability and fractional plasma volume once the time dependence of Gd-DTPA concentration in blood is known. In the present study, we have limited the analysis to the empirical measurement of the AUC because the time dependence of Gd-DTPA in blood was not known and not easily measurable. At this point, we cannot state if the effect on AUC values is determined by a decrease in permeability to Gd-DTPA or in blood volume, although the observation that no alterations in blood volume were detected with the macromolecular contrast agent could mean that the permeability to the low molecular weight contrast agent is altered.

Early MRI findings are correlated to the classical end point of tumor size reduction at later time points; in fact, it has been reported that daily administration of 40 mg/kg of SU11248 produces a substantial regression (by 62%) of the tumor size compared with the size at the beginning of therapy in HT-29 human colon carcinoma implanted s.c. in nude mice (9).

To the best of our knowledge, this is the first report on the evaluation of antiangiogenic activity of SU11248 *in vivo* by DCE-MRI. Considering that DCE-MRI done with Gd-DTPA can be exported to clinics, the present findings could be relevant for the design of clinical trials based on new paradigms.

References

1. Cristofanilli M, Cristofanilli M, Charnsangavej C, Hortobagyi GN. Angiogenesis modulation in cancer research: novel clinical approaches. Nat Rev Drug Discov 2002;1:415–26.
2. Choyke PL, Dwyer AJ, Knopp MV. Functional tumor imaging with dynamic contrast-enhanced magnetic resonance imaging. J Magn Reson Imaging 2003;17:509–20.
3. Padhani AR. Dynamic contrast-enhanced MRI in clinical oncology: current status and future directions. J Magn Reson Imaging 2002;16:407–22.
4. Gossmann A, Okuhata Y, Shames DM, et al. Prostate cancer tumor grade differentiation with dynamic contrast-enhanced MR imaging in the rat: comparison of macromolecular and small-molecular contrast media-preliminary experience. Radiology 1999;213:265–72.
5. Roberts TP, Turetschek K, Preda A, et al. Tumor microvascular changes to anti-angiogenic treatment assessed by MR contrast media of different molecular weights. Acad Radiol 2002;9 Suppl 2:S511–3.
6. Turetschek K, Preda A, Novikov V, et al. Tumor microvascular changes in antiangiogenic treatment: assessment by magnetic resonance contrast media of different molecular weights. J Magn Reson Imaging 2004;20:138–44.
7. Marzola P, Degrassi A, Calderan L, et al. *In vivo* assessment of antiangiogenic activity of SU6668 in an experimental colon carcinoma model. Clin Cancer Res 2004;10:739–50.
8. Turetschek K, Huber S, Floyd E, et al. MR imaging characterization of microvessels in experimental breast tumors by using a particulate contrast agent with histopathologic correlation. Radiology 2001;218:562–9.
9. Mendel DB, Mendel DB, Laird AD, et al. *In vivo* antitumor activity of SU11248, a novel tyrosine kinase inhibitor targeting vascular endothelial growth factor and platelet-derived growth factor receptors: determination of a pharmacokinetic/pharmacodynamic relationship. Clin Cancer Res 2003;9:327–37.
10. Abrams TJ, Murray LJ, Pesenti E, et al. Preclinical evaluation of the tyrosine kinase inhibitor SU11248 as a single agent and in combination with "standard of care" therapeutic agents for the treatment of breast cancer. Mol Cancer Ther 2003;2:1011–21.
11. O'Farrell AM, Abrams TJ, Yuen HA, et al. SU11248 is a novel FLT3 tyrosine kinase inhibitor with potent activity *in vitro* and *in vivo*. Blood 2003;101:3597–605.
12. Daldrup H, Shames DM, Wendland M, et al. Correlation of dynamic contrast-enhanced magnetic resonance imaging with histological tumor grade: comparison of macromolecular and small molecular contrast media. Pediatr Radiol 1998;28:67–78.
13. Ogan MD, Schmiedl U, Moseley ME, Grodd W, Paajanen H, Brasch RC. Albumin labeled with Gd-DTPA. An intravascular contrast-enhancing agent for magnetic resonance blood pool imaging: preparation and characterization. Invest Radiol 1987;22:665–71.
14. Marzola P, Farace P, Calderan, et al. *In vivo* mapping of fractional plasma volume (fPV) and endothelial transfer coefficient (kPS) in solid tumors using a macromolecular contrast agent: correlation with histology and ultrastructure. Int J Cancer 2003;104:462–8.
15. Morgan B, Thomas AL, Drevs J, et al. Dynamic contrast-enhanced magnetic resonance imaging as a biomarker for the pharmacological response of PTK787/ZK 222584, an inhibitor of the vascular endothelial growth factor receptor tyrosine kinases, in patients with advanced colorectal cancer and liver metastases: results from two phase I studies. J Clin Oncol 2003;21:3955–64.
16. Morimoto AM, Tan N, West K, et al. Gene expression profiling of human colon xenograft tumors following treatment with SU11248, a multitargeted tyrosine kinase inhibitor. Oncogene 2004;23:1618–26.
17. Robinson SP, McIntyre DJ, Checkley D, et al. Tumour dose response to the antivascular agent ZD6126 assessed by magnetic resonance imaging. Br J Cancer 2003;88:1592–7.
18. Weissleder R, Bogdanov A Jr, Tung CH, Weinmann HJ. Size optimization of synthetic graft copolymers for *in vivo* angiogenesis imaging. Bioconjug Chem 2001;12:213–9.
19. Turetschek K, Floyd E, Helbich T, et al. MRI assessment of microvascular characteristics in experimental

breast tumors using a new blood pool contrast agent (MS-325) with correlations to histopathology. J Magn Reson Imaging 2001;14:237–42.

20. Turetschek K, Roberts TP, Floyd E, et al. Tumor microvascular characterization using ultrasmall superparamagnetic iron oxide particles (USPIO) in an experimental breast cancer model. Magn Reson Imaging 2001;13:882–8.

21. Turetschek K, Preda A, Floyd E, et al. MRI monitoring of tumor response to a novel VEGF tyrosine kinase inhibitor in an experimental breast cancer model. Acad Radiol 2002;9:S519–20.

22. Turetschek K, Preda A, Floyd E, et al. MRI monitoring of tumor response following angiogenesis inhibition in an experimental human breast cancer model. Eur J Nucl Med Mol Imaging 2003;30:448–55.

23. Drevs J, Muller-Driver R, Wittig C, et al. PTK787/ZK 222584, a specific vascular endothelial growth factor-receptor tyrosine kinase inhibitor, affects the anatomy of the tumor vascular bed and the functional vascular properties as detected by dynamic enhanced magnetic resonance imaging. Cancer Res 2002;62:4015–22.

24. Bhujwalla ZM, Artemov D, Natarajan K, Solaiyappan M, Kollars P, Kristjansen PE. Reduction of vascular and permeable regions in solid tumors detected by macromolecular contrast magnetic resonance imaging after treatment with antiangiogenic agent TNP-470. Clin Cancer Res 2003;9:355–62.

Clinical Cancer Research

Early Antiangiogenic Activity of SU11248 Evaluated *In vivo* by Dynamic Contrast-Enhanced Magnetic Resonance Imaging in an Experimental Model of Colon Carcinoma

Pasquina Marzola, Anna Degrassi, Laura Calderan, et al.

Clin Cancer Res 2005;11:5827-5832.